Geophysical Research Letters

RESEARCH LETTER
10.1002/2018GL077261

Key Points:
- Cloud fraction and optical thickness of in situ formed ice clouds increase monotonically and sharply with aerosol loading
- These properties of anvil ice clouds increase with small aerosol loading but decrease with further aerosol increase
- The impacts of various aerosol types on properties of anvil ice clouds are substantially different

Supporting Information:
- Supporting Information S1

Correspondence to:
B. Zhao and Y. Gu,
zhaob1206@ucla.edu;
gu@atmos.ucla.edu

Citation:
Zhao, B., Gu, Y., Liou, K.-N., Wang, Y., Liu, X., Huang, L., et al. (2018). Type-dependent responses of ice cloud properties to aerosols from satellite retrievals. *Geophysical Research Letters*, *45*, 3297–3306. https://doi.org/10.1002/2018GL077261

Received 22 JAN 2018
Accepted 24 MAR 2018
Accepted article online 30 MAR 2018
Published online 13 APR 2018

Type-Dependent Responses of Ice Cloud Properties to Aerosols From Satellite Retrievals

Bin Zhao[1,2], Yu Gu[1], Kuo-Nan Liou[1], Yuan Wang[2,3], Xiaohong Liu[4], Lei Huang[1,2], Jonathan H. Jiang[2], and Hui Su[2]

[1]Joint Institute for Regional Earth System Science and Engineering and Department of Atmospheric and Oceanic Sciences, University of California, Los Angeles, CA, USA, [2]Jet propulsion Laboratory, California Institute of Technology, Pasadena, CA, USA, [3]Division of Geological and Planetary Sciences, California Institute of Technology, Pasadena, CA, USA, [4]Department of Atmospheric Science, University of Wyoming, Laramie, WY, USA

Abstract Aerosol-cloud interactions represent one of the largest uncertainties in external forcings on our climate system. Compared with liquid clouds, the observational evidence for the aerosol impact on ice clouds is much more limited and shows conflicting results, partly because the distinct features of different ice cloud and aerosol types were seldom considered. Using 9-year satellite retrievals, we find that, for convection-generated (anvil) ice clouds, cloud optical thickness, cloud thickness, and cloud fraction increase with small-to-moderate aerosol loadings (<0.3 aerosol optical depth) and decrease with further aerosol increase. For in situ formed ice clouds, however, these cloud properties increase monotonically and more sharply with aerosol loadings. An increase in loading of smoke aerosols generally reduces cloud optical thickness of convection-generated ice clouds, while the reverse is true for dust and anthropogenic pollution aerosols. These relationships between different cloud/aerosol types provide valuable constraints on the modeling assessment of aerosol-ice cloud radiative forcing.

Plain Language Summary Aerosol-cloud interactions represent one of the largest uncertainties in external forcings on our climate system. Compared with liquid clouds, the observational evidence for the aerosol impact on ice clouds is much more limited and shows conflicting results, partly because the distinct features of different ice cloud and aerosol types were seldom considered. Using 9-year satellite retrievals, we find that the responses of ice cloud properties to aerosols differ according to the types of cloud/aerosols. For convection-generated (anvil) ice clouds, the thickness, optical thickness, and amount of clouds increase with small-to-moderate aerosol loadings and decrease with further aerosol increase. For in situ formed ice clouds, however, these cloud properties increase monotonically and more sharply with aerosol loadings. An increase in loading of smoke aerosols generally reduces the optical thickness of convection-generated ice clouds, while the reverse is true for dust and anthropogenic pollution aerosols. These relationships between different cloud/aerosol types provide valuable constraints on the modeling assessment of aerosol-ice cloud radiative forcing.

1. Introduction

Ice clouds, which consist only of ice crystals and are primarily cirrus clouds, cover over 30% of the Earth's surface (Wylie et al., 1994, 2005) and substantially modulate global radiation budget (Liou, 1986, 2005). They cool the Earth by reflecting solar radiation and heat the Earth by trapping longwave terrestrial radiation (Chen et al., 2000; Fu & Liou, 1993; Liou, 1986, 2005). Ice clouds also contribute to the dehydration of air as they enter the stratosphere and modulate the balance of water vapor between the lower stratosphere and upper troposphere (Fu et al., 2006; Jensen et al., 1996; Jensen, Diskin, et al., 2013).

The formation of ice clouds involves homogeneous nucleation of solution droplets formed on cloud condensation nuclei at temperatures below about −35°C, as well as heterogeneous nucleation processes involving certain aerosol types acting as ice nucleating particles (Hoose & Moehler, 2012; Intergovernmental Panel on Climate Change (IPCC), 2013; Seinfeld et al., 2016). In contrast to extensive studies on the aerosol impact on liquid and mixed-phase clouds (IPCC, 2013; Rosenfeld et al., 2014; Zhao, Liou, et al., 2017), the connections between aerosols and ice clouds have received much less attention and remain poorly understood. Limited available modeling studies reported that the global radiative forcing due to aerosol-ice cloud interactions ranged between $-0.67\ W/m^{-2}$ and $0.70\ W/m^{-2}$ (Fan et al., 2016; IPCC, 2013; Liu et al., 2009), representing one of the largest uncertainties in anthropogenic forcings on our climate system.

In order to reduce the above substantial uncertainty, it is imperative to conduct systematic observational analysis for evidence of the aerosol impact on ice cloud properties. However, the aerosol effects on ice clouds have been difficult to constrain due to numerous controlling factors. Moreover, limited available studies have shown contradicting results (Chylek et al., 2006; Huang et al., 2006; Jiang et al., 2008; Ou et al., 2009; Patel & Kumar, 2016; Su et al., 2011; Tesche et al., 2016; W. C. Wang et al., 2015). For example, Huang et al. (2006) and W. C. Wang et al. (2015) showed that the existence of dust aerosols significantly lower cloud optical thickness (COT) and ice water path (IWP) of ice clouds compared with pristine conditions, whereas a number of studies (Ou et al., 2009; Patel & Kumar, 2016; Tesche et al., 2016) reported a significant increase in COT and/or IWP with an increase in dust aerosols or aircraft exhaust. While the causes for the disagreement and uncertainty are not yet clear, the distinct characteristics of different ice cloud and aerosol types under various meteorological conditions could presumably lead to different aerosol-ice cloud relationships. Two major ice cloud types with distinct formation pathways have been differentiated in previous studies (Kramer et al., 2016; Mace et al., 2006, 2001): (1) ice clouds generated by the detrainment of deep convective clouds (convection-generated ice clouds, also called anvil ice clouds) and (2) those formed in situ as a result of frontal systems, orographic or gravity waves (i.e., in situ formed ice clouds). In addition, absorbing and nonabsorbing aerosols have been found to have different impacts on the vertical development of deep convective clouds (Massie et al., 2016; Ramanathan et al., 2005; Rosenfeld et al., 2008), which could subsequently affect the properties of ice clouds detrained from them. To the best of our knowledge, none of the previous observational studies has investigated or compared the impact of various aerosol types on the physical properties of the two ice cloud types.

In this study, we investigate the interactions of aerosols and ice clouds using 9-year satellite retrievals, taking into consideration different ice cloud and aerosol types. Consistent with the work of Zhao et al. (2018), the study region is over East Asia (70°–135°E, 15°–55°N), in which there are substantial anthropogenic emissions (Wang et al., 2014) and the aerosol loadings span a large range and the aerosol types are diverse as a function of time and locations (Wang et al., 2017; Zhao, Jiang, et al., 2017).

2. Data and Methodology

2.1. Sources and Collocation of Satellite Retrievals

We use collocated satellite retrievals of aerosol and cloud properties from CALIOP (Cloud-Aerosol Lidar with Orthogonal Polarization) aboard Cloud-Aerosol Lidar and Infrared Pathfinder Satellite Observations, CloudSat, and MODIS (Moderate Resolution Imaging Spectroradiometer) aboard Aqua, as summarized in Table S1 in the supporting information.

We select the CALIOP profiles with single-layer ice clouds and valid quality assurance (QA) flags based on the CALIOP 05kmMLay product (V4.10) at a 5 km along-track resolution. A cloud layer is identified as ice cloud (i.e., cloud consisting only of ice) if its layer base temperature is colder than −35°C or its "cloud type" is "cirrus." The cloud thickness and COT are taken directly from the 05kmMLay product. Subsequently, we match collocated aerosol/cloud measurements from all sensors to the CALIOP 5-km profiles. The ice cloud fraction (ICF) is calculated using the ratio of the number of 1×1 km MODIS overcast cloud pixels (MYD06 product, collection 6) for which the "primary cloud retrieval outcome" is successful and the "cloud phase" is ice to the number of all pixels within a 20-km radius of a CALIOP profile, following the method used to calculate ICF in level 3 MODIS products (Hubanks et al., 2016). We only include in ICF calculation the MODIS pixels that vertically overlap with the CALIOP ice cloud layer (layer top pressure of CALIOP ice cloud layer—10 hPa $\leq$ cloud top pressure of MODIS ice pixel $\leq$ layer base pressure of CALIOP ice cloud layer), in order to minimize contamination by the cloud pixels that does not belong to the same cloud layer as detected by CALIOP. Through a number of sensitivity test, we have shown that the modification in ICF calculation method does not noticeably affect the response of ICF to aerosol loading (see Text S1). The ice water content (IWC) and IWP from a CloudSat-CALIOP combined product (2C-ICE, version P1_R04) are matched to CALIOP profiles by averaging 2C-ICE profiles at about 1.7-km along-track resolution within the range of a CALIOP 5-km profile. The IWC data are also vertically averaged between the top and bottom of the ice cloud layer retrieved by CALIOP (see more discussions about IWC retrievals in Text S2).

For aerosol optical depth (AOD), considering that MODIS AOD retrievals are usually missing in cloudy scenes and that this study inevitably needs to sample AOD near clouds, we average AOD pixels (MYD04 product,

collection 6) at 10 × 10 km resolution within a 30-km radius from CALIOP profiles to increase the quantity of valid AOD samples. The spatially averaged AOD should provide a good approximation of that at the location of the CALIOP profile considering the large spatial length scale (40–400 km) of AOD variation (Anderson et al., 2003). Besides column AOD, we derive AOD of aerosol layers that overlap the CALIOP ice cloud layer (i.e., layer AOD) by averaging AOD of each overlapping aerosol layer (from 05kmMLay product) within a 30-km radius from the CALIOP profile. CALIOP-retrieved aerosol and ice cloud layers are considered to overlap if they are vertically $<$0.25 km apart from each other and have valid QA flags (Costantino & Breon, 2010). We then eliminate profiles with column AOD $>$ 1.5 or layer AOD $>$ 0.7 to reduce the cloud contamination effect (F. Wang et al., 2015). While the filters applied in this study (single-layer cloud, CALIOP QA flags, AOD range, etc.) are necessary to ensure the quality of the data samples, a caveat is that they may potentially bias the distribution of the samples. In subsequent analysis, we use the column AOD and layer AOD to represent the aerosol loadings that interact with convection-generated and in situ formed ice clouds, respectively, since in situ ice clouds mainly depend on high-altitude aerosols while convection-generated ice clouds could also be affected by lower-altitude aerosols lifted by convective updraft. When evaluating the aerosol impact on all types of ice clouds as a whole, we use column AOD following previous studies (e.g., Jiang et al., 2011; Massie et al., 2007; Ou et al., 2009; Zhao et al., 2018). Note that we use column AOD data from MODIS rather than CALIOP, because a much smaller number of valid AOD samples are available from CALIOP in case of convection-generated ice clouds due to its narrow swath. Also, the near-surface aerosol retrievals from CALIOP are subject to large uncertainty because of undetected surface attached aerosols as well as surface contamination (NASA CALIPSO team, 2011).

To evaluate the impact of meteorology on aerosol-ice cloud interactions, we achieve vertically resolved relative humidity from the CALIOP 05kmAPro product (V4.10) and a number of meteorological variables (summarized in Table S1) from the Final Analysis reanalysis data product of National Centers for Environmental Prediction with 1° × 1° and 6-hr resolutions. A CALIOP profile is assigned the meteorological parameters of the corresponding National Centers for Environmental Prediction's grid at 06:00 UTC, which is closest to the satellite overpass time between 5:00 and 8:00 UTC.

2.2. Determination of Ice Cloud and Aerosol Types

We distinguish convection-generated and in situ formed ice clouds based primarily on their connection to deep convection clouds, using the CALIOP 05kmMLay product and the approach applied in our previous study (Zhao et al., 2018). In brief, convection-generated ice clouds are composed of ice cloud profiles that are connected to deep convection profiles. Two neighboring CALIOP cloud layers are considered to be "connected" if they vertically overlap and their horizontal distance is $\leq$5 km. Note that convection-generated ice clouds, also called anvil ice clouds, are the anvil detrained from deep convective clouds rather than the deep convective core. In contrast, in situ ice cloud must not contain any deep convection profiles and must consist of connected ice cloud profiles which are at least 25 km in horizontal direction.

Zhao et al. (2018) have presented the probability distributions of COT and cloud thickness of these two ice cloud types and found that COT and cloud thickness of convection-generated ice clouds (44.9% of all profiles) are significantly larger compared to in situ formed ice clouds (52.4% of all profiles), which is in good consistency with many aircraft measurements (e.g., Kramer et al., 2016; Muhlbauer et al., 2014). Therefore, the ice cloud type classification appears to be reasonable despite some imperfections.

Finally, to evaluate the impact of different aerosol types on ice clouds, we group all selected profiles according to the "aerosol type" flag from the CALIOP 05kmMLay product. The aerosol types identified include dust, polluted dust, clean continental aerosols, polluted continental aerosols, and smoke. We merge clean continental aerosols and polluted continental aerosols into "anthropogenic pollution aerosols" following Rosenfeld et al. (2011), as these two types are composed of similar chemical constituents originating from anthropogenic activities, including SO_4^{2-}, NO_3^-, NH_4^+, and organic matter (NASA CALIPSO team, 2012). The profiles with different aerosol types for different aerosol layers are grouped into "multiple type."

3. Results and Discussion

3.1. Overall Impact of Aerosols on Ice Cloud Properties

Figure 1a shows the overall responses of ice cloud properties to aerosol loadings, with all ice cloud and aerosol types lumped together. For small-to-moderate aerosol loadings (AOD $<$ 0.3), cloud thickness, COT, and ICF all

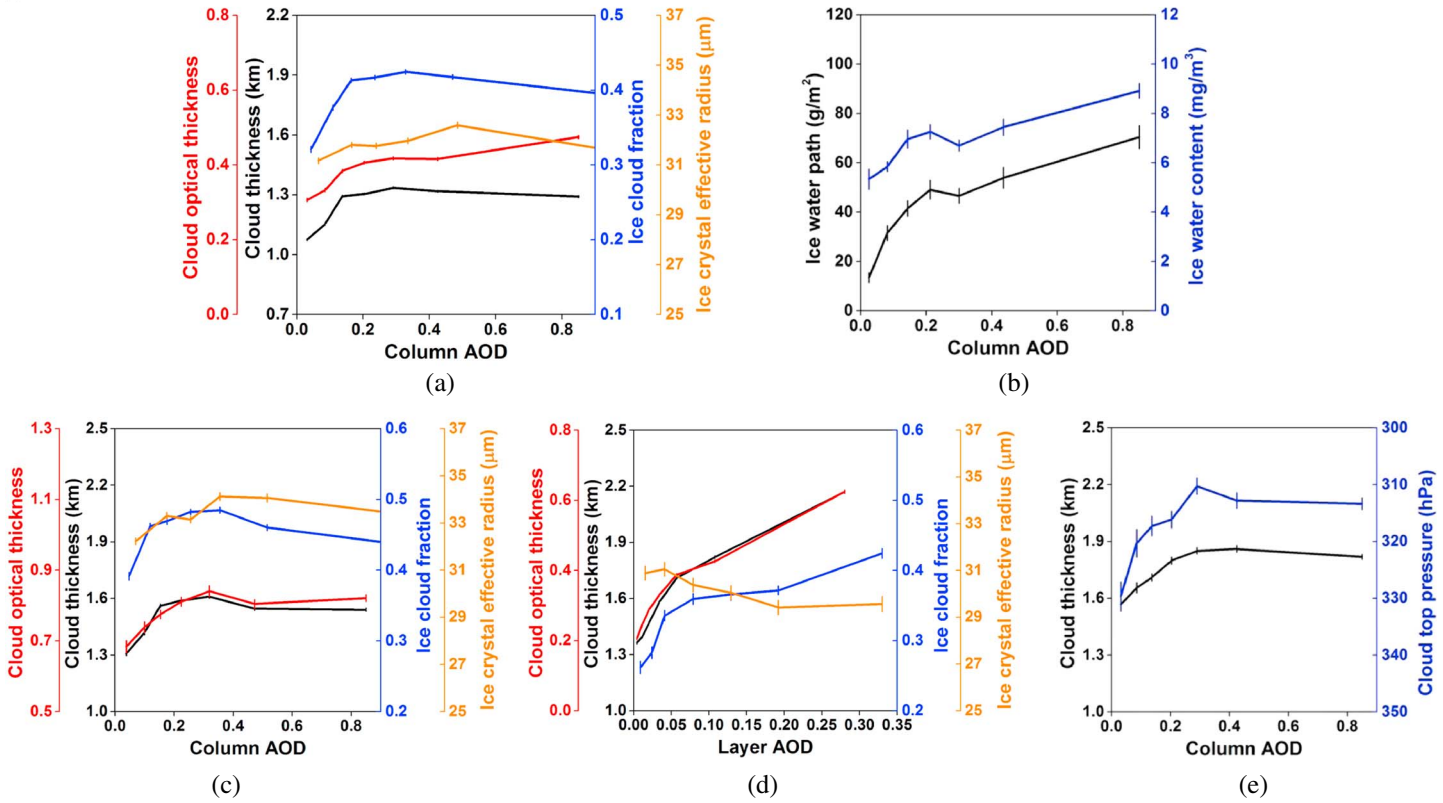

Figure 1. Changes in the properties of (a, b) all ice cloud types, (c) anvil ice clouds, (d) in situ ice clouds, and (e) deep convective clouds that anvil ice clouds are connected to, with column/layer aerosol optical depth (AOD). Note that anvil ice clouds are the anvil detrained from deep convective clouds rather than the deep convective core. The deep convective clouds shown in (e) are not the target of this study and are illustrated only to facilitate the interpretation of the aerosol impact on anvil ice clouds. The AOD bins are selected so that each bin contains a similar number of samples. The error bars represent the standard errors ($\sigma/\sqrt{N}$), where N is the sample number and σ is the standard deviation. The total numbers of samples used in the figures are 2.8×10^5, 5.7×10^4, and 9.8×10^4 for cloud optical thickness, ice cloud fraction (ICF)/ice crystal effective radius (R_{ei}), and ice water path/ice water content of all ice cloud types, 6.2×10^4 and 2.7×10^4 for cloud thickness/cloud optical thickness and ICF/R_{ei} of anvil ice clouds, 2.3×10^5 and 1.1×10^4 for cloud thickness/cloud optical thickness and ICF/R_{ei} of in situ ice clouds, and 1.7×10^4 for deep convective clouds.

increase rapidly with increasing AOD. For higher aerosol loadings, however, the trends are much weaker: COT increases slightly with AOD, while cloud thickness and ICF level off or decreases slightly. To give a quantitative assessment, we group all data samples into three equal AOD subsets, with the lowest third labeled as "clean" and the highest third labeled as "polluted." The average cloud thickness, COT, and ICF increase by 11%, 31%, and 12%, respectively, from the clean to the polluted groups (Table S2). For reference, the IWP and IWC measured by CloudSat also show similar trends with the increase in AOD, as shown in Figure 1b.

The relationships described above do not indicate causality. A possible explanation for the positive correlations could be that the same meteorological conditions that favor the development of ice clouds also favor higher aerosol loadings. To exclude this possibility, we restrict the meteorological variation and analyze aerosol-cloud correlations as a function of the meteorological range. Among the meteorological variables that may significantly influence ice cloud development, relative humidity averaged between 100 and 440 hPa ($RH_{100\text{-}440hPa}$) and pressure vertical velocity at 300 hPa (VV300) correlate best with major ice cloud properties (see Table S3). Therefore, we plot the relationships between AOD and ice cloud properties (cloud thickness, COT, and ICF) for different ranges of $RH_{100\text{-}440hPa}$ (Figures 2a–2c) and VV300 (Figures S2a–S2c). The relationship patterns are similar in different meteorological ranges, implying that meteorological covariations are unlikely major causes for these relationships. We also perform the same analysis for other meteorological parameters in Table S3 and find similar results (not shown). We also bin cloud thickness/COT/ICF according to $RH_{100\text{-}440hPa}$ and VV300, for different AOD ranges (Figures 2d–2f and S2d–S2f). Using $RH_{100\text{-}440hPa}$ and cloud thickness as an example, for any given $RH_{100\text{-}440hPa}$, an increase in AOD always enlarges cloud thickness, demonstrating the role of aerosols in increasing cloud thickness regardless of this meteorological

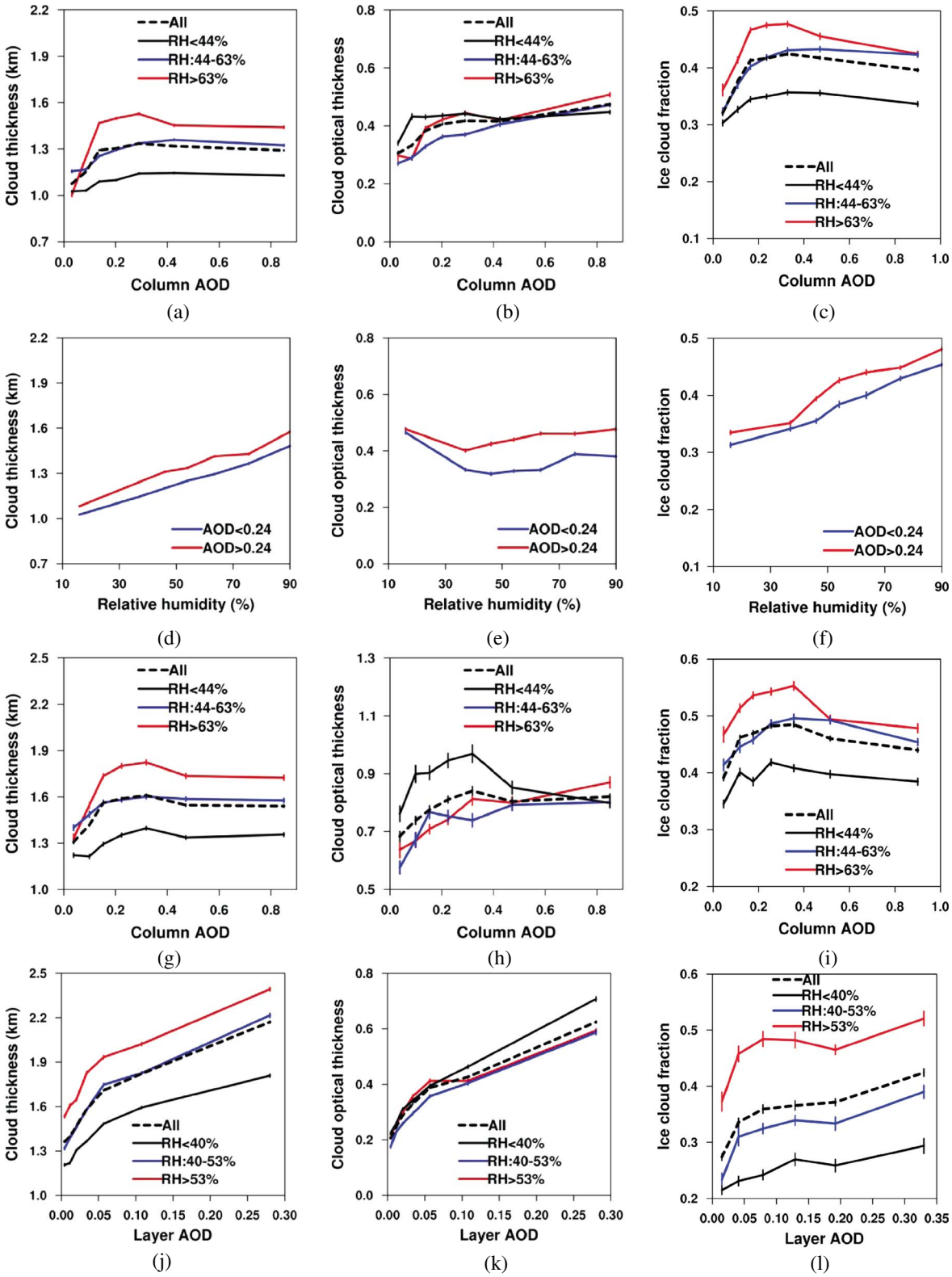

Figure 2. Influence of relative humidity on the responses of ice cloud properties to aerosol loadings. (a–c) Changes in (a) cloud thickness, (b) cloud optical thickness (COT), and (c) ice cloud fraction (ICF) with column aerosol optical depth (AOD) under three subsets of relative humidity averaged between 100 and 440 hPa ($RH_{100\text{-}440hPa}$). (d–f) Changes in (d) cloud thickness, (e) COT, and (f) ICF with $RH_{100\text{-}440hPa}$ for different AOD ranges. (g–i) Similar to (a)–(c) but for properties of convection-generated (anvil) ice clouds. (j–l) Similar to (a)–(c) but for the changes of the properties of in situ ice clouds with layer AOD. We divide AOD and meteorological variables and into two and three ranges, respectively, each containing a similar sample number. The error bar definition is the same as in Figure 1.

parameter. The same results are also shown for VV300 and for COT/ICF. In addition, we find that AOD does not show large variations in response to changes in any meteorological variable considered in this study (see Text S3 for details). Furthermore, we have calculated the partial correlation between column/layer AOD and ice cloud properties following Engstrom and Ekman (2010). The partial correlation is a measure of the linear dependence between two variables where the influence from possible controlling variables (meteorological parameters in this case) is removed (Engstrom & Ekman, 2010; Johnson & Wichern, 2007; PSU, 2017). The partial correlations are generally similar to total correlations, indicating that meteorological covariations at reanalysis data resolution do not appear to be a major cause for the correlations between aerosols and ice cloud properties (see Text S3 for details).

Moreover, we demonstrate that contamination of AOD retrievals by clouds (Kaufman et al., 2005) is unlikely to result in the preceding aerosol-cloud relationships (see Text S4). Also, we find that the uncertainty magnitude in the retrievals of COT, ICF, cloud thickness, and AOD is generally much smaller than the ice cloud property trends in response to AOD (see Text S5). For these reasons, we conclude that the aerosol-ice cloud relationships are significantly attributed to the aerosol effects.

3.2. Impact of Aerosols on Two Types of Ice Clouds

In Figures 1c and 1d, we plot changes in ice cloud properties with aerosol loadings separately for two ice cloud types. For convection-generated ice clouds, cloud thickness, COT, and ICF increase significantly with small-to-moderate AODs of <0.3. At larger AODs these physical properties, especially cloud thickness and ICF, show decreasing trends when AOD increases, though the rates of decrease are still significantly smaller than the increasing rates at smaller AOD range. A similar "boomerang shape" relationship has been previously reported for warm clouds by Koren et al. (2008). For in situ ice clouds, however, the preceding properties all increase monotonically and more sharply with layer AOD. As a quantitative comparison, for convection-generated ice clouds, the average cloud thickness, COT, and ICF of the polluted group defined in section 3.1 (i.e., the highest third AOD) are only 8%, 11%, and 5% higher than those of the clean subset (the lowest third AOD), whereas the corresponding fractional differences are as high as 42%, 113%, and 37% for in situ ice clouds (Table S2).

Similar to the preceding section, we find that the relationships between cloud thickness/COT/ICF and column/layer AOD are generally quite similar under different ranges of $RH_{100\text{-}440hPa}$ (Figures 2g–2l) and VV300 (S2g–S2l), for either ice cloud type. The COT-aerosol relationships for convection-generated ice clouds are subject to large fluctuations probably because COT could be more affected by a number of microphysical processes such as depositional growth, aggregation, and sedimentation, which are sensitive to environmental conditions. Nevertheless, the general pattern still remains such that within any meteorological range, COT increases noticeably with small AODs, and stabilizes or decreases at larger AODs. These results reinforce our conclusion that the correlations between aerosols and ice clouds are significantly attributed to the aerosol effect.

To interpret the aerosol impact on anvil ice clouds, we first examine changes in the properties of deep convective clouds they are physically connected to (Figure 1e). The cloud thickness and cloud top height (negatively correlated with cloud top pressure) of the deep convective clouds increase substantially with small-to-moderate AODs (<0.3) and subsequently stabilize and decrease slightly. This is consistent with the findings of Rosenfeld et al. (2008) that an AOD increase at small AODs invigorates deep convection through the hypothesized "invigoration effect" (additional latent heat release due to freezing of a larger amount of cloud water) but could inhibit convection at larger AODs, which decrease the amount of sunlight reaching the surface and reduce the buoyancy by delaying the sedimentation of ice crystals. The invigoration and inhibition of convection by aerosols at small/large AOD ranges could subsequently lead to the increase/decrease in cloud thickness/COT/ICF of anvil ice clouds detrained from them at the corresponding AOD ranges. In addition, the heating and evaporation of ice crystals due to solar radiation absorption by aerosols may also contribute to the decrease in cloud thickness/COT/ICF at large AODs, consistent with the findings of Koren et al. (2008) for warm clouds.

With respect to in situ ice clouds, we propose that an increase in aerosols enlarges cloud thickness/COT/ICF by enhancing ice crystal formation and changing sedimentation rate. As shown in Zhao et al. (2018), the formation of in situ ice clouds can be dominated by either homogeneous or heterogeneous nucleation. When

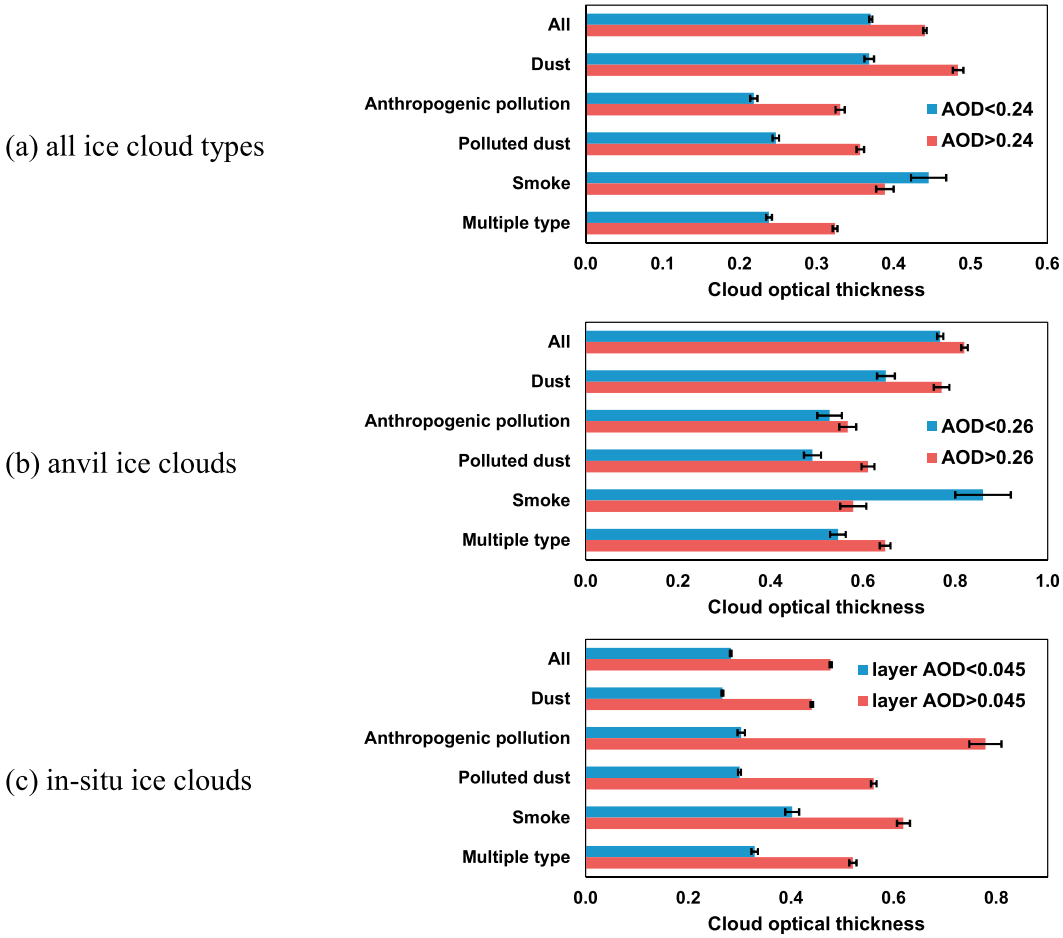

Figure 3. The cloud optical thickness (COT) in high and low aerosol optical depth (AOD) subsets for different aerosol types identified by Cloud-Aerosol Lidar with Orthogonal Polarization: (a) all ice cloud types, (b) convection-generated (anvil), and (c) in situ formed ice clouds. Two subsets of column AOD/layer AOD used here contain similar sample number. The differences between the COT under high and low AODs are statistically significant at the 0.01 level based on the Student's *t* test except for two cases: For all ice cloud types with smoke aerosols, the difference is significant at the 0.05 level, while for convection-generated ice clouds with anthropogenic pollution, the difference is not significant. The error bar definition is the same as in Figure 1.

homogeneous nucleation dominates, Zhao et al. (2018) show that R_{ei} decreases rapidly with aerosols due to the production of a larger quantity of smaller ice crystals; therefore, the sedimentation rate is reduced and the ice water amount becomes larger. This resembles the aerosol indirect effect on liquid clouds (Albrecht, 1989; Liou & Ou, 1989). If heterogeneous nucleation dominates, R_{ei} is not sensitive to aerosol loading (see Figures 3d–3f of Zhao et al., 2018), because the ice supersaturation ratio surrounding ice crystals is usually quite high (up to ~70%) and does not noticeably limit their growth (Jensen, Diskin, et al., 2013; Kramer et al., 2009). As a result, more aerosols (and thus more ice nucleating particles, such as dust and glassy organic aerosols) would produce more ice crystals and hence larger ice water amount. In addition, because in situ formed ice clouds are mainly influenced by tenuous aerosol layers near the cloud altitudes, the aerosol absorption effect, which plays an important role only at large aerosol loadings (Koren et al., 2008), should be insufficient to offset the microphysical effect. That is why cloud thickness/COT/ICF show monotonically increasing trends with aerosols rather than boomerang shape trends. Although the aerosol effects illustrated in this study can be reasonably interpreted, we need to further support these explanations as well as quantify the relative importance of different processes using process-level measurements and numerical modeling in future studies.

3.3. Impact of Different Aerosol Types

Figure 3 shows the impact of different aerosol types identified by CALIOP on COT of convection-generated and in situ formed ice clouds, as well as all cloud types. Here we divide the samples of each aerosol type

into two-column AOD/layer AOD subsets in order to increase the number of samples in each subset. For convection-generated ice clouds (Figure 3b), the higher AOD subset is associated with larger COT when the aerosol types are dust, anthropogenic pollution, polluted dust, or multiple type. With reference to smoke, COT of the high AOD subset is substantially smaller than that of the low AOD subset. The differences between the two AOD subsets are all statistically significant at the 0.01 level, except for the anthropogenic pollution case. The inhibition effect of smoke could be explained by the fact that smoke, as compared to other aerosol types, consists of a larger fraction of absorbing aerosols (Dubovik et al., 2002), such as black carbon and light-absorbing organic aerosol (Kirchstetter & Thatcher, 2012), which could accelerate evaporation of ice crystals through absorptive heating, as discussed in section 3.2. Moreover, absorbing aerosols have been found to stabilize the temperature profile and suppress convection (Ramanathan et al., 2005, 2007), which may subsequently inhibit the detrainment of convection-generated ice clouds.

In terms of in situ ice clouds (Figure 3c), an increase in layer AOD of any aerosol type results in statistically significant increase in COT. This is probably because the layer AOD affecting in situ ice clouds is usually quite small; therefore, aerosols' microphysical effect which elevates COT generally far exceeds the effect of absorptive heating that reduces COT. The fractional increases in COT from low to high AOD ranges are the largest for anthropogenic pollution aerosols (about 150%), probably because the number concentration of anthropogenic pollution aerosols is larger than other aerosol types for a given AOD. When the two ice cloud types are lumped together (Figure 3a), COT is lower in the high AOD subset for smoke aerosols, whereas the reverse is true for other aerosol types.

4. Conclusions and Implications

In this study, we investigated the impact of different aerosol types on the properties of two types of ice clouds using 9-year satellite retrievals. Overall cloud thickness, COT, and ICF, increase rapidly with small-to-moderate AODs ($<$0.3) and generally level off at higher aerosol loadings. The aerosol impacts on ice cloud properties are significantly different for convection-generated and in situ formed ice clouds. The cloud thickness, COT, and ICF of convection-generated ice clouds increase significantly when AOD $<$ 0.3, probably because of the aerosol-induced invigoration of deep convection that generates the ice clouds; these physical properties decrease with AOD at larger aerosol loadings likely attributable to the absorptive evaporation of ice crystals and inhibition of deep convection. For in situ ice clouds, however, the preceding cloud properties increase monotonically and more sharply with aerosol loading, since aerosols' microphysical effect dominates over absorption effect. When aerosols are decomposed into different types, the higher AOD subsets of dust, anthropogenic pollution aerosols, and polluted dust are associated with larger COT of convection-generated ice clouds than the lower AOD subsets, while the reverse is true for smoke aerosols, which is probably due to a larger fraction of absorbing aerosols and hence enhanced absorptive evaporation and inhibition of convection. In contrast, an increase in any aerosol type can significantly enlarge COT of in situ ice clouds.

The physical properties of ice clouds, including cloud thickness, COT, and ICF, determine their infrared greenhouse (warming) effect and solar albedo (cooling) effect, as well as the balance between the two. We demonstrate that ice cloud properties respond significantly to aerosol loadings. The response is especially strong at relatively small AOD range (column AOD $<$ 0.25; Figure 1a). The occurrence frequency of this AOD range is about 53%, and the related clouds account for about 45% of the total cloud cover. More importantly, we provide the first-ever evidence that these responses of ice clouds differs significantly in both sign and magnitude, according to the types of ice clouds and aerosols. These findings appear to be important for understanding and reconciling the conflicting observational results concerning the aerosol effects on ice cloud properties. Moreover, the cloud/aerosol type-dependent relationships derived in this study can be used to evaluate and constrain atmospheric models so as to resolve the causes for the contradictory model estimates of aerosol-ice cloud radiative forcing ($-$0.67 to 0.70 W/m^{-2}; Fan et al., 2016; IPCC, 2013; Liu et al., 2009) and subsequently improve the model assessment of aerosol-ice cloud interactions.

While the present study focuses on the impact of aerosols, we acknowledge that other ice processes such as ice crystal growth by vapor deposition and aggregation, ice multiplication, and ice sedimentation can affect the ice particle size/shape and number concentrations, and hence ice cloud macrophysical properties (Jensen, Lawson, et al., 2013; Jensen et al., 2012; Kay et al., 2006; Lawson et al., 2015). Quantifying the

relative contributions of aerosols and other cloud controlling processes to ice cloud variations is an important task which merits further in-depth studies.

Acknowledgments
This study is supported by the NSF grant AGS-1701526, the UCLA Grand Challenge grant 50958, and NASA ROSES CCST and TASNPP grants. XL acknowledges the support of NSF grant AGS-1642289. We acknowledge the support of the Jet Propulsion Laboratory, California Institute of Technology, under contract with NASA, and the Joint Institute for Regional Earth System Science and Engineering in the University of California Los Angeles. All data needed to evaluate the conclusions in the paper are present in the paper and/or the supporting information. Additional data related to this paper can be requested from the authors.

References

Albrecht, B. A. (1989). Aerosols, cloud microphysics, and fractional cloudiness. *Science*, *245*(4923), 1227–1230. https://doi.org/10.1126/science.245.4923.1227

Anderson, T. L., Charlson, R. J., Winker, D. M., Ogren, J. A., & Holmen, K. (2003). Mesoscale variations of tropospheric aerosols. *Journal of the Atmospheric Sciences*, *60*(1), 119–136. https://doi.org/10.1175/1520-0469(2003)060%3C0119:MVOTA%3E2.0.CO;2

Chen, T., Rossow, W. B., & Zhang, Y. C. (2000). Radiative effects of cloud-type variations. *Journal of Climate*, *13*(1), 264–286. https://doi.org/10.1175/1520-0442(2000)013%3C0264:REOCTV%3E2.0.CO;2

Chylek, P., Dubey, M. K., Lohmann, U., Ramanathan, V., Kaufman, Y. J., Lesins, G., et al. (2006). Aerosol indirect effect over the Indian Ocean. *Geophysical Research Letters*, *33*, L06806. https://doi.org/10.1029/2005GL025397

Costantino, L., & Breon, F. M. (2010). Analysis of aerosol-cloud interaction from multi-sensor satellite observations. *Geophysical Research Letters*, *37*, L11801. https://doi.org/10.1029/2009GL041828

Dubovik, O., Holben, B., Eck, T. F., Smirnov, A., Kaufman, Y. J., King, M. D., et al. (2002). Variability of absorption and optical properties of key aerosol types observed in worldwide locations. *Journal of the Atmospheric Sciences*, *59*(3), 590–608. https://doi.org/10.1175/1520-0469(2002)059%3C0590:VOAAOP%3E2.0.CO;2

Engstrom, A., & Ekman, A. M. L. (2010). Impact of meteorological factors on the correlation between aerosol optical depth and cloud fraction. *Geophysical Research Letters*, *37*, L18814. https://doi.org/10.1029/2010GL044361

Fan, J. W., Wang, Y., Rosenfeld, D., & Liu, X. H. (2016). Review of aerosol–cloud interactions: Mechanisms, significance, and challenges. *Journal of the Atmospheric Sciences*, *73*(11), 4221–4252. https://doi.org/10.1175/JAS-D-16-0037.1

Fu, Q., Johanson, C. M., Wallace, J. M., & Reichler, T. (2006). Enhanced mid-latitude tropospheric warming in satellite measurements. *Science*, *312*(5777), 1179–1179.

Fu, Q., & Liou, K. N. (1993). Parameterization of the radiative properties of cirrus clouds. *Journal of the Atmospheric Sciences*, *50*(13), 2008–2025. https://doi.org/10.1175/1520-0469(1993)050%3C2008:POTRPO%3E2.0.CO;2

Hoose, C., & Moehler, O. (2012). Heterogeneous ice nucleation on atmospheric aerosols: A review of results from laboratory experiments. *Atmospheric Chemistry and Physics*, *12*(20), 9817–9854. https://doi.org/10.5194/acp-12-9817-2012

Huang, J. P., Minnis, P., Lin, B., Wang, T. H., Yi, Y. H., Hu, Y. X., et al. (2006). Possible influences of Asian dust aerosols on cloud properties and radiative forcing observed from MODIS and CERES. *Geophysical Research Letters*, *33*, L06824. https://doi.org/10.1029/2005GL024724

Hubanks, P., Platnick, S., King, M., & Ridgway, B. (2016). MODIS atmosphere L3 pridded product Algorithm Theoretical Basis Document (ATBD) & users guide.

Intergovernmental Panel on Climate Change (IPCC) (2013). Climate change 2013: The physical science basis. In *Contribution of Working Group I to the Fifth Assessment Report of the Intergovernmental Panel on Climate Change* (chap. 7, 1535 pp.). Cambridge, UK and New York: Cambridge University Press.

Jensen, E. J., Diskin, G., Lawson, R. P., Lance, S., Bui, T. P., Hlavka, D., et al. (2013). Ice nucleation and dehydration in the tropical tropopause layer. *Proceedings of the National Academy of Sciences of the United States of America*, *110*(6), 2041–2046. https://doi.org/10.1073/pnas.1217104110

Jensen, E. J., Lawson, R. P., Bergman, J. W., Pfister, L., Bui, T. P., & Schmitt, C. G. (2013). Physical processes controlling ice concentrations in synoptically forced, midlatitude cirrus. *Journal of Geophysical Research: Atmospheres*, *118*, 5348–5360. https://doi.org/10.1002/jgrd.50421

Jensen, E. J., Pfister, L., & Bui, T. P. (2012). Physical processes controlling ice concentrations in cold cirrus near the tropical tropopause. *Journal of Geophysical Research*, *117*, D11205. https://doi.org/10.1029/2011JD017319

Jensen, E. J., Toon, O. B., Selkirk, H. B., Spinhirne, J. D., & Schoeberl, M. R. (1996). On the formation and persistence of subvisible cirrus clouds near the tropical tropopause. *Journal of Geophysical Research*, *101*(D16), 21,361–21,375. https://doi.org/10.1029/95JD03575

Jiang, J. H., Su, H., Schoeberl, M. R., Massie, S. T., Colarco, P., Platnick, S., & Livesey, N. J. (2008). Clean and polluted clouds: Relationships among pollution, ice clouds, and precipitation in South America. *Geophysical Research Letters*, *35*, L14804. https://doi.org/10.1029/2008GL034631

Jiang, J. H., Su, H., Zhai, C., Massie, S. T., Schoeberl, M. R., Colarco, P. R., et al. (2011). Influence of convection and aerosol pollution on ice cloud particle effective radius. *Atmospheric Chemistry and Physics*, *11*(2), 457–463. https://doi.org/10.5194/acp-11-457-2011

Johnson, R. A., & Wichern, D. W. (2007). *Applied multivariate statistical analysis* (6th ed.). NJ: Pearson Education Inc.

Kaufman, Y. J., Koren, I., Remer, L. A., Rosenfeld, D., & Rudich, Y. (2005). The effect of smoke, dust, and pollution aerosol on shallow cloud development over the Atlantic Ocean. *Proceedings of the National Academy of Sciences of the United States of America*, *102*(32), 11,207–11,212. https://doi.org/10.1073/pnas.0505191102

Kay, J. E., Baker, M., & Hegg, D. (2006). Microphysical and dynamical controls on cirrus cloud optical depth distributions. *Journal of Geophysical Research*, *111*, D24205. https://doi.org/10.1029/2005JD006916

Kirchstetter, T. W., & Thatcher, T. L. (2012). Contribution of organic carbon to wood smoke particulate matter absorption of solar radiation. *Atmospheric Chemistry and Physics*, *12*(14), 6067–6072. https://doi.org/10.5194/acp-12-6067-2012

Koren, I., Martins, J. V., Remer, L. A., & Afargan, H. (2008). Smoke invigoration versus inhibition of clouds over the Amazon. *Science*, *321*(5891), 946–949. https://doi.org/10.1126/science.1159185

Kramer, M., Rolf, C., Luebke, A., Afchine, A., Spelten, N., Costa, A., et al. (2016). A microphysics guide to cirrus clouds—Part 1: Cirrus types. *Atmospheric Chemistry and Physics*, *16*(5), 3463–3483. https://doi.org/10.5194/acp-16-3463-2016

Kramer, M., Schiller, C., Afchine, A., Bauer, R., Gensch, I., Mangold, A., et al. (2009). Ice supersaturations and cirrus cloud crystal numbers. *Atmospheric Chemistry and Physics*, *9*(11), 3505–3522. https://doi.org/10.5194/acp-9-3505-2009

Lawson, R. P., Woods, S., & Morrison, H. (2015). The microphysics of ice and precipitation development in tropical cumulus clouds. *Journal of the Atmospheric Sciences*, *72*(6), 2429–2445. https://doi.org/10.1175/JAS-D-14-0274.1

Liou, K. N. (1986). Influence of cirrus clouds on weather and climate processes—A global perspective. *Monthly Weather Review*, *114*(6), 1167–1199. https://doi.org/10.1175/1520-0493(1986)114%3C1167:IOCCOW%3E2.0.CO;2

Liou, K. N. (2005). *Cirrus clouds and climate in McGraw-Hill Yearbook of Science and Technology*. New York: McGraw-Hill Professional.

Liou, K. N., & Ou, S. C. (1989). The role of cloud microphysical processes in climate—An assessment from a one-dimensional perspective. *Journal of Geophysical Research*, *94*(D6), 8599–8607. https://doi.org/10.1029/JD094iD06p08599

Liu, X. H., Penner, J. E., & Wang, M. H. (2009). Influence of anthropogenic sulfate and black carbon on upper tropospheric clouds in the NCAR CAM3 model coupled to the IMPACT global aerosol model. *Journal of Geophysical Research*, *114*, D03204. https://doi.org/10.1029/2008JD010492

Mace, G. G., Benson, S., & Vernon, E. (2006). Cirrus clouds and the large-scale atmospheric state: Relationships revealed by six years of ground-based data. *Journal of Climate*, *19*(13), 3257–3278. https://doi.org/10.1175/JCLI3786.1

Mace, G. G., Clothiaux, E. E., & Ackerman, T. P. (2001). The composite characteristics of cirrus clouds: Bulk properties revealed by one year of continuous cloud radar data. *Journal of Climate*, *14*(10), 2185–2203. https://doi.org/10.1175/1520-0442(2001)014%3C2185:TCCOCC%3E2.0.CO;2

Massie, S. T., Delano, J., Bardeen, C. G., Jiang, J. H., & Huang, L. (2016). Changes in the shape of cloud ice water content vertical structure due to aerosol variations. *Atmospheric Chemistry and Physics*, *16*(10), 6091–6105. https://doi.org/10.5194/acp-16-6091-2016

Massie, S. T., Heymsfield, A., Schmitt, C., Muller, D., & Seifert, P. (2007). Aerosol indirect effects as a function of cloud top pressure. *Journal of Geophysical Research*, *112*, D06202. https://doi.org/10.1029/2006JD007383

Muhlbauer, A., Ackerman, T. P., Comstock, J. M., Diskin, G. S., Evans, S. M., Lawson, R. P., & Marchand, R. T. (2014). Impact of large-scale dynamics on the microphysical properties of midlatitude cirrus. *Journal of Geophysical Research: Atmospheres*, *119*, 3976–3996. https://doi.org/10.1002/2013JD020035

NASA CALIPSO team (2011). CALIPSO quality statements lidar level 3 aerosol profile monthly products version release: 1.00.

NASA CALIPSO team (2012). CALIPSO quality statements lidar level 2 cloud and aerosol layer products version releases: 3.01, 3.02.

Ou, S. S. C., Liou, K. N., Wang, X. J., Hansell, R., Lefevre, R., & Cocks, S. (2009). Satellite remote sensing of dust aerosol indirect effects on ice cloud formation. *Applied Optics*, *48*(3), 633–642.

Patel, P. N., & Kumar, R. (2016). Dust induced changes in ice cloud and cloud radiative forcing over a high altitude site. *Aerosol and Air Quality Research*, *16*(8), 1820–1831. https://doi.org/10.4209/aaqr.2015.05.0325

PSU (2017). STAT 505—Applied multivariate statistical analysis. Retrieved from https://onlinecourses.science.psu.edu/stat505/node/

Ramanathan, V., Chung, C., Kim, D., Bettge, T., Buja, L., Kiehl, J. T., et al. (2005). Atmospheric brown clouds: Impacts on South Asian climate and hydrological cycle. *Proceedings of the National Academy of Sciences of the United States of America*, *102*(15), 5326–5333. https://doi.org/10.1073/pnas.0500656102

Ramanathan, V., Ramana, M. V., Roberts, G., Kim, D., Corrigan, C., Chung, C., & Winker, D. (2007). Warming trends in Asia amplified by brown cloud solar absorption. *Nature*, *448*(7153), 575–578. https://doi.org/10.1038/nature06019

Rosenfeld, D., Andreae, M. O., Asmi, A., Chin, M., de Leeuw, G., Donovan, D. P., et al. (2014). Global observations of aerosol-cloud-precipitation-climate interactions. *Reviews of Geophysics*, *52*, 750–808. https://doi.org/10.1002/2013RG000441

Rosenfeld, D., Lohmann, U., Raga, G. B., O'Dowd, C. D., Kulmala, M., Fuzzi, S., et al. (2008). Flood or drought: How do aerosols affect precipitation? *Science*, *321*(5894), 1309–1313. https://doi.org/10.1126/science.1160606

Rosenfeld, D., Yu, X., Liu, G., Xu, X., Zhu, Y., Yue, Z., et al. (2011). Glaciation temperatures of convective clouds ingesting desert dust, air pollution and smoke from forest fires. *Geophysical Research Letters*, *38*, L21804. https://doi.org/10.1029/2011GL049423

Seinfeld, J. H., Bretherton, C., Carslaw, K. S., Coe, H., DeMott, P. J., Dunlea, E. J., et al. (2016). Improving our fundamental understanding of the role of aerosol-cloud interactions in the climate system. *Proceedings of the National Academy of Sciences of the United States of America*, *113*(21), 5781–5790. https://doi.org/10.1073/pnas.1514043113

Su, H., Jiang, J. H., Lu, X. H., Penner, J. E., Read, W. G., Massie, S., et al. (2011). Observed increase of TTL temperature and water vapor in polluted clouds over Asia. *Journal of Climate*, *24*(11), 2728–2736.

Tesche, M., Achtert, P., Glantz, P., & Noone, K. J. (2016). Aviation effects on already-existing cirrus clouds. *Nature Communications*, *7*, 12016. https://doi.org/10.1038/ncomms12016

Wang, F., Guo, J. P., Zhang, J. H., Huang, J. F., Min, M., Chen, T. M., et al. (2015). Multi-sensor quantification of aerosol-induced variability in warm clouds over eastern China. *Atmospheric Environment*, *113*, 1–9. https://doi.org/10.1016/j.atmosenv.2015.04.063

Wang, J., Zhao, B., Wang, S., Yang, F., Xing, J., Morawska, L., et al. (2017). Particulate matter pollution over China and the effects of control policies. *The Science of the Total Environment*, *584*, 426–447.

Wang, S. X., Zhao, B., Cai, S. Y., Klimont, Z., Nielsen, C. P., Morikawa, T., et al. (2014). Emission trends and mitigation options for air pollutants in East Asia. *Atmospheric Chemistry and Physics*, *14*, 6571–6603. https://doi.org/10.5194/acp-14-6571-2014

Wang, W. C., Sheng, L. F., Jin, H. C., & Han, Y. Q. (2015). Dust aerosol effects on cirrus and altocumulus clouds in northwest China. *Journal of Meteorological Research*, *29*(5), 793–805. https://doi.org/10.1007/s13351-015-4116-9

Wylie, D. P., Jackson, D. L., Menzel, W. P., & Bates, J. J. (2005). Trends in global cloud cover in two decades of HIRS observations. *Journal of Climate*, *18*(15), 3021–3031. https://doi.org/10.1175/JCLI3461.1

Wylie, D. P., Menzel, W. P., Woolf, H. M., & Strabala, K. I. (1994). 4 years of global cirrus cloud statistics using Hirs. *Journal of Climate*, *7*(12), 1972–1986. https://doi.org/10.1175/1520-0442(1994)007%3C1972:FYOGCC%3E2.0.CO;2

Zhao, B., Jiang, J. H., Gu, Y., Diner, D., Worden, J., Liou, K. N., et al. (2017). Decadal-scale trends in regional aerosol particle properties and their linkage to emission changes. *Environmental Research Letters*, *12*(5), 054021. https://doi.org/10.1088/1748-9326/aa6cb2

Zhao, B., Liou, K. N., Gu, Y., Jiang, J. H., Li, Q., Fu, R., et al. (2018). Impact of aerosols on ice crystal size. *Atmospheric Chemistry and Physics*, *18*(2), 1065–1078. https://doi.org/10.5194/acp-18-1065-2018

Zhao, B., Liou, K. N., Gu, Y., Li, Q., Jiang, J. H., Su, H., et al. (2017). Enhanced PM2.5 pollution in China due to aerosol-cloud interactions. *Scientific Reports*, *7*(1), 4453. https://doi.org/10.1038/s41598-017-04096-8